Determining the Effect of Residual SWI/SNF Subunits on Small Cell Carcinoma of the Ovary Hypercalcemic Type (SCCOHT) Cell Lines

By

Cassandra Perrone

A Thesis Submitted in Partial Fulfillment of the Requirements for the Degree of Master of Science in Biology

Middle Tennessee State University

May 2024

Thesis Committee:

April Weissmiller, Ph.D., Chair

Jason Jessen, Ph.D.

Frank Bailey, Ph.D.

ACKNOWLEDGEMENTS

I wanted to thank my outstanding family and friends for all the love and support throughout my academic career at MTSU. Without their encouragement, I would not be where I am today. Mom, Dad, Nick, Marc, Nana, Poppop, Grandma, Marjorie, Shelby, and Max: I love you all with my whole heart! Thank you for pushing me to reach for the stars.

I am also thankful for all the graduate students whom I shared this journey with. We did it! I am so very proud of us. Further, I would like to give a major shout out to my outstanding mentor Dr. April Weissmiller. Thank you for absolutely everything you have done for me within the last two years. I cannot explain how much I appreciate your guidance and sharing of knowledge with me throughout my graduate career. I have learned many new techniques as well as skills in and out of the laboratory which I will be forever grateful for. To the Weissmiller Lab: thank you all for the fun times shared together and all the help in the laboratory to make this project complete. I deeply appreciate Dr. Jason Jessen and Dr. Frank Bailey for taking the time and effort to be on my thesis committee. Thank you for all the encouraging feedback and guidance throughout the thesis writing process.

I am giving a big thank you to the Graduate Scholarship Committee for awarding me the John Patten Scholarship, J.L. Fletcher Scholarship, and the 2023 Summer Stipend. These awards provided me with finances for laboratory supplies as well as living expenses throughout my research career.

ABSTRACT

Small cell carcinoma of the ovary, hypercalcemic type (SCCOHT) is a rare and aggressive cancer which has an exceptionally high mortality rate. The main mutation correlated with this cancer type impacts the proper functioning of a major chromatin remodeling complex called SWI/SNF. One commonality of all SCCOHT cancers is deleterious mutation of the *SMARCA4* gene that is known to encode for the SWI/SNF ATPase subunit, BRG1. Loss of BRG1 incorporation within SWI/SNF is the driving mutational event to promote tumorigenesis, and it has been difficult to find new therapy options for patients with this type of cancer, resulting in a low survival rate. In other cancers defined by SWI/SNF subunit mutations like SCCOHT, there is a reliance of the cancer state on the SWI/SNF subunits that remain present in the cell. Two proteins with important functions in the SWI/SNF chromatin remodeling complexes that remain following BRG1 loss are BAF155 and ARID1A. To investigate whether these two remaining SWI/SNF subunits are important for SCCOHT cancer processes, I determined in my thesis work whether knockdown in expression levels of these SWI/SNF subunits has any detrimental impact on SCCOHT cell proliferation and cell cycle progression. To achieve this, I introduced a new CRISPR technique called CRISPR interference (CRISPRi) into the laboratory to target BAF155 and ARID1A subunit expression. Results from this research indicate that CRISPRi worked more successfully for targeting knockdown of BAF155. However, in contrast to my hypothesis, decreasing BAF155 levels did not impair cell division but rather induced a trend towards increased cell function. Overall, my thesis research has provided insight into the dependency of SCCOHT cell lines on a core SWI/SNF subunit and helped to define the optimal parameters for future CRISPRi-based research in the laboratory that will assist the uncovering of essential proteins in various cancer cell lines.

TABLE OF CONTENTS

TABLE OF FIGURES

INTRODUCTION

Small Cell Carcinoma of the Ovary Hypercalcemic Type (SCCOHT)

Small cell carcinoma of the ovary, hypercalcemic type (SCCOHT) is a rare ovarian malignancy that is aggressive in nature. This cancer type affects young women with an average age of 24 years (1). Current treatment comprises of surgery (complete hysterectomy) as well as multiple rounds of chemotherapy and radiation. Histologic characteristics consist of small cells of unknown origin with scant cytoplasm packed into sheets with a diffuse-like pattern (2). Common symptoms leading up to diagnosis consist of abdominal pain, bloating, weight loss, nausea, and constipation (1). Additionally, hypercalcemia is found in around two thirds of SCCOHT patients after diagnosis (2). SCCOHT patients diagnosed in Stage 1 typically have a survival rate of 33%, but diagnosis beyond this stage generally leads to death (3). Around 65% of SCCOHT patients have recurrence of the cancer within 12 months of remission and unfortunately succumb to the disease within two years of diagnosis, averaging at 16 months (1). SCCOHT cancers typically have one major biological characteristic in common: mutations in SWI/SNF chromatin remodeling complexes.

SWI/SNF

SWI/SNF chromatin remodeling complexes are important in eukaryotic cells, where genomic DNA is compacted into chromatin within the nucleus; chromatin specifically is DNA that is wrapped around proteins known as histones to form nucleosomes that then get tightly wound together to form chromosomes (4). Chromosomes are the structures in which DNA is stored in cells. To fix, replicate, or transcribe portions of DNA, the use of a chromatin remodeling complex is needed (5). There are four major chromatin remodeling complexes, but one of the most well-studied is SWI/SNF. SWI/SNF complexes use the energy of ATP hydrolysis to manipulate the histone:DNA interactions and contain 10-14 different subunits, giving SWI/SNF complexes their unique functions shown in Figure 1 (4, 5).

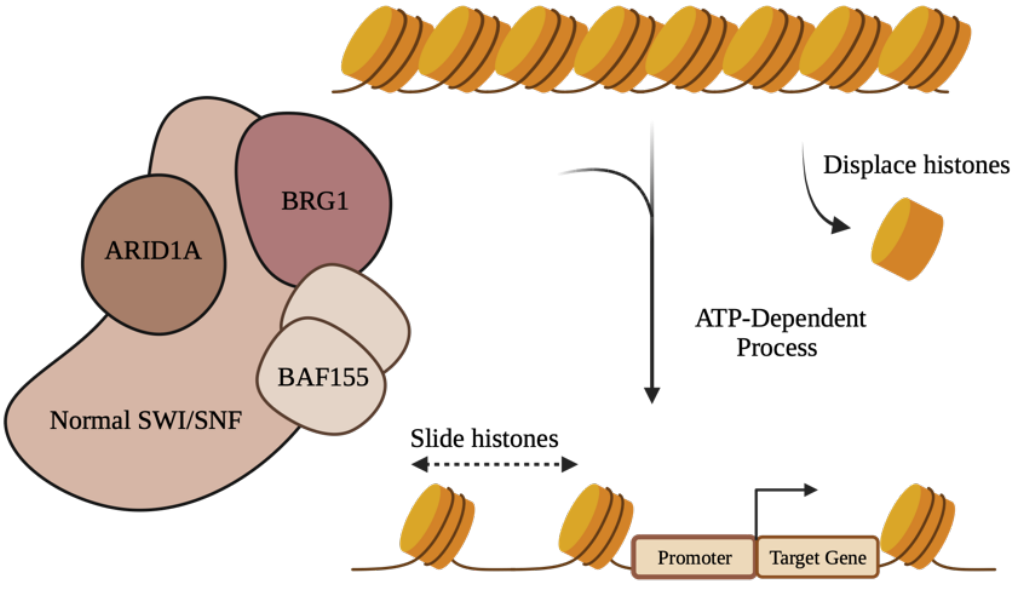

Figure 1. The SWI/SNF chromatin remodeling complex. *SWI/SNF is a chromatin remodeling complex that uses ATP hydrolysis to move histone proteins along DNA. This process allows for target genes to be accessed by important proteins, such as RNA polymerase, which are needed for the transcription process to occur. This figure was made using BioRender.*

There are three types of mammalian SWI/SNF complexes called canonical BAF (cBAF), non-canonical BAF (ncBAF), and polybromo-associated BAF (pBAF), defined by their unique subunit compositions and the region of the genome they are thought to regulate (4). However, all the mammalian SWI/SNF complexes have a mutually exclusive ATPase subunit: either BRG1 (*SMARCA4* gene encodes BRG1 protein) or BRM (*SMARCA2* gene encodes BRM protein). Mutations can occur within the genes that encode the specific subunits of SWI/SNF complexes, and around 25% of all cancers have one or more SWI/SNF subunit mutations (4). Examples of various SWI/SNF gene mutations in cancers are as follows: *SMARCB1* mutation is typically found in malignant rhabdoid tumor (MRT), *PBRM1* mutation is typically found in renal cell carcinoma, and *ARID2* mutation is typically found in malignant melanoma as well as urothelial bladder carcinoma (4, 6). *SMARCA4* mutation is typically found in Burkitt's lymphoma, medulloblastoma, and as I describe below, SCCOHT (4, 6). Many of these mutations are loss-of-function, meaning the gene mutation results in the protein being reduced or completely abolished in production, and, thus, SWI/SNF complex function is altered.

SCCOHT is one of many cancers that is defined by SWI/SNF subunit mutation (5). Nearly all SCCOHT cancers show mutation to the *SMARCA4* gene, which encodes the main ATPase subunit, called BRG1, resulting in loss of BRG1 in the cell (7). As *SMARCA2* is unexpressed in SCCOHT through unknown epigenetic reasons (8), it is thought that these cancers are driven by dual ATPase loss. However, how loss of SWI/SNF ATPase function results in this deadly cancer is still unknown, and it is also unclear the mechanisms at work to allow SCCOHT to thrive in its cancer state. What is

known, however, is that the reintroduction of BRG1 into SCCOHT cell lines can restore SWI/SNF function regarding tumor suppression and gene regulation (7, 9). These data imply that when BRG1 is lost, normal SWI/SNF function is impaired and regulation of the genome by SWI/SNF complexes becomes altered. Unfortunately, a therapy that reintroduces ATPase function in SCCOHT is currently not feasible, so continued studies to uncover the cancerous pathways working in BRG1-null cancers like SCCOHT are needed.

Residual SWI/SNF as a Target in SWI/SNF-Altered Cancers

One interesting feature about cancers marked by SWI/SNF subunit mutation is that the subunits that remain present following particular SWI/SNF subunit loss can form abnormal SWI/SNF complexes (called "residual" SWI/SNF herein). In many cancers marked by SWI/SNF subunit mutation, it has been proven that residual SWI/SNF complexes maintain the cancer state by facilitating expression of genes involved in oncogenic pathways such as growth, protein synthesis, migration, and signaling (7, 10) rather than those linked to development and differentiation. For some of these cancers, residual SWI/SNF subunits that remain can be synthetic lethal targets in terms of cancer treatment. Synthetic lethality is a phenomenon that can occur between two genes when mutation occurs where a deleterious mutation of one gene causes dependence of another gene that otherwise would not occur in the cell. Typically, synthetic lethals exist in a mutually exclusive fashion where only one gene is expressed at a time, not both. For example, in ARID1A-null cancer cells, ARID1B is incorporated into an aberrant residual SWI/SNF complex. However, when ARID1B levels are knocked down using short

hairpin RNA (shRNA), the cancer cells stop proliferating, so ARID1B would be a synthetic lethal target in the residual complex (11). A similar synthetic lethality exists in BRG1-null cancer cells in that the loss of BRG1 leads to a dependency on the BRM subunit, but targeting BRM by shRNA approaches a reduction in cell growth (8).

The most similar type of SWI/SNF-altered cancer to SCCOHT, on a biological and histological level, is malignant rhabdoid tumor (MRT), which, as mentioned above, is defined by *SMARCB1* mutation. MRT is a rare and aggressive childhood cancer that occurs in infants and children (6). Histologically, MRT is considered a small celled aggressive neoplasm similar to SCCOHT (6), revealing they have common pathologies. The *SMARCB1* gene that encodes the SNF5 protein (6) is a validated tumor suppressor that, among many cellular activities, interacts with the TP53 protein responsible for regulating cell cycle (12). Like other cancers in which SWI/SNF subunit expression is altered, in MRT, there is also an accepted synthetic lethal SWI/SNF subunit target, known as BRD9. BRD9 is known to be responsible for regulating cell proliferation as well as having a bromodomain that allows for the chromatin remodeling complex to be recruited to specific locations in chromatin (13). Bromodomains can identify acetyl groups on proteins, which, therefore, marks chromatin binding sites for the remodeling and modifying complexes to bind DNA (13). To impact the expression of the synthetic lethal target, BRD9, in MRT Michel *et al*. used two separate techniques to achieve sufficient knockdown expression of the gene: shRNA as well as a degrader (dBRD9) which inhibit expression of BRD9 by tagging the protein for degradation in the cell. Observed cell proliferation and cell cycle changes occurred after sufficient knockdown of BRD9, supporting the idea that BRD9 is an essential subunit for *SMARCB1*-null cancers,

such as MRT, and can possibly be a synthetic lethal therapy target therapeutically (14). In sum, the evidence across multiple SWI/SNF-altered cancers supports the idea that residual SWI/SNF subunits are potential targets in cancers marked by SWI/SNF subunit mutation. Because of these data, it is possible that targeting essential proteins in the residual SWI/SNF chromatin remodeling complex is worthwhile; however, it is currently unclear if SWI/SNF subunits are synthetic lethal targets in this cancer and what role the residual SWI/SNF complex has in maintaining SCCOHT cancer cell function.

As it relates to SCCOHT, which is the focus of this project, identification of retained SWI/SNF complexes upon loss of BRG1 have been observed (7) - an example of this is shown in Figure 2. The complex, as mentioned already, also does not contain the other ATPase, BRM, suggesting that these residual SWI/SNF complexes may not actively remodel chromatin as their primary function but may have some other function for the cell. If the oncogenic and cancerous pathways regulated by residual SWI/SNF in SCCOHT are understood, new targeted therapies for these types of cancers may be discovered, which could increase the length of survival for SCCOHT patients. However, there has been little investigation into how residual SWI/SNF subunits affect SCCOHT cancer cells and if any SWI/SNF subunits could serve as new targets for these types of cancers. Therefore, the goal of my research is to see whether SCCOHT cancers rely on remaining residual SWI/SNF subunits to achieve the important cancer function of being able to grow and divide.

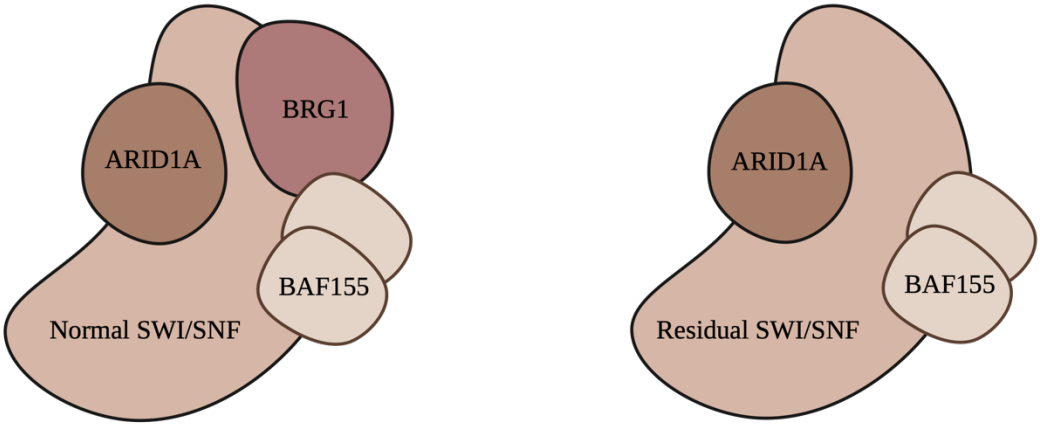

Figure 2. Residual SWI/SNF formed from SMARCA4 mutation*. This diagram shows the comparison between "normal" SWI/SNF chromatin remodeling complex and mutated residual SWI/SNF chromatin remodeling complex formed from the loss of BRG1 encoded by the SMARCA4 gene. This figure was made using BioRender.*

Gene Manipulation Through CRISPR and CRISPRi

To understand how a gene contributes to a measurable phenotype, such as cell growth and division, techniques that perturb the level of the gene product in the cell are routinely employed. A new contemporary approach to disrupting the level of gene products in the cell is called CRISPR. CRISPR stands for "Clustered Regularly Interspaced Short Palindromic Repeats" which is innovative technology used for genomic editing (15). This tool provides a precise and efficient technique for scientists to make changes to a genome and depends on the CRISPR-Cas9 complex which acts as "genetic scissors" to cause gene knockouts or edits (15). In the CRISPR system, Cas9 can recognize and cleave specific nucleic acids of target using single guide RNA (sgRNA) that anneals to the DNA target of interest (15). These sgRNA sequences act as a guide for Cas9 protein to cleave nucleic acids with high specificity. The Cas9 protein used in the CRISPR-Cas9 system contains two major protein domains called the HNH and RuvC

domains, which, together, cleave the double strands of DNA (15) (Figure 3). This system was revolutionary in the world of genetics due to its versatility and feasibility; therefore, this system has been altered to use for various purposes.

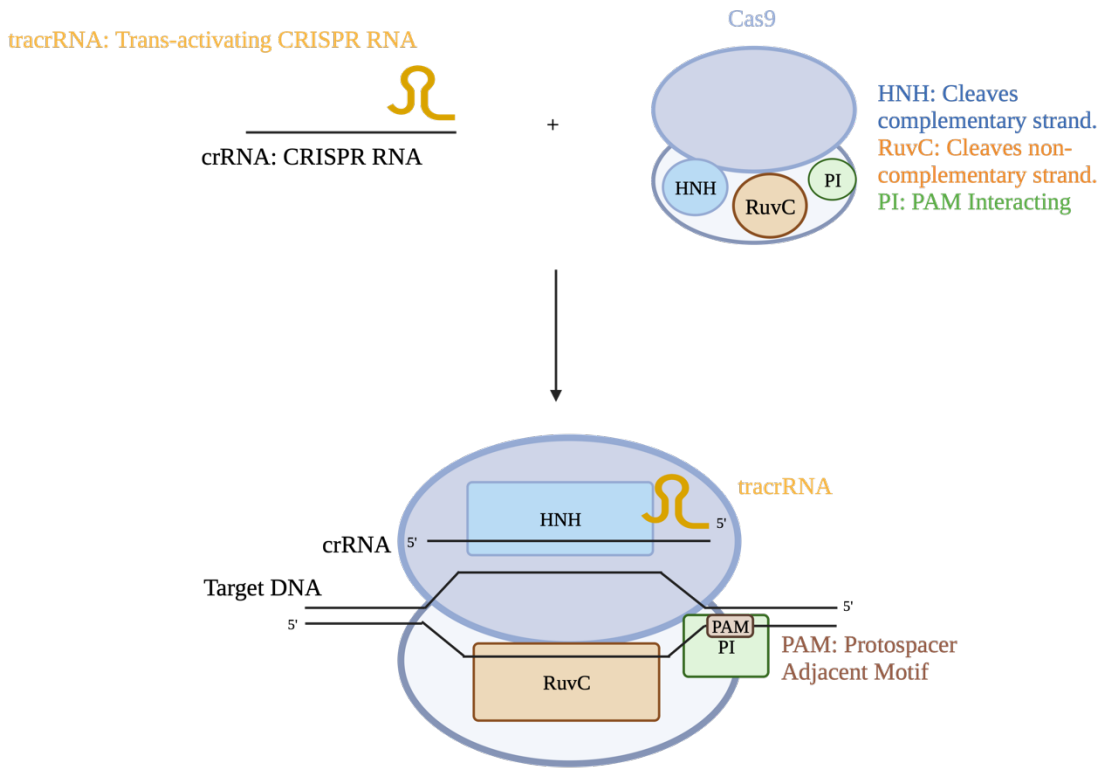

Figure 3. Clustered Regularly Interspaced Short Palindromic Repeats (CRISPR) Cas9 complex for genome editing. *The top left diagram represents the single guide RNA that is used by Cas9 (to the right) to scan target DNA for the complementary match and the PAM sequence. Once found, the HNH and RuvC domains can cleave foreign nucleic acids. This figure was made using BioRender.*

CRISPR is the major method used by researchers to knockout function of a gene or to make precise edits to genes. However, more recently, a new type of CRISPR technology to emerge in the scientific field is CRISPRi which stands for CRISPR "interference" (15). This technique allows researchers the ability to knockdown expression of a gene rather than remove its expression completely. This is an important

contribution to gene manipulation techniques because some genes are essential, and they cannot be totally removed from the cell for the cell to survive for scientific investigation. By having a method to knockdown expression of a gene, CRISPRi has opened more flexibility in study of gene function and it's more akin to shRNA approaches, which were early techniques to study gene function well. The major difference between CRISPR and CRISPRi is that Cas9 is catalytically dead (dCas9) due to single point mutations made within the HNH and RuvC domains. These point mutations prevent Cas9 from cleaving double stranded DNA, although Cas9 can still bind through sgRNA-guided targeting (16) (Figure 4). The Cas9 used in CRISPRi is a chimeric protein that is fused to the Kruppel-associated box (KRAB) domain which is part of the zinc finger protein family of transcriptional regulators (17). KRAB domains within KRAB proteins normally function to repress gene expression by recruiting corepressors such as KAP1, which acts as a scaffolding protein (18) to assemble the interaction of various chromatin regulators such as HP1α (Heterochromatin Protein 1) and the recruitment of histone methyltransferases (17). The specific histone that gets trimethylated is the ninth lysine residue of histone three (H3K9me3), causing tighter wrapping of DNA around the histone protein (17, 19). Trimethylation of these specific histone residues causes recruitment of HP1α, which then induces the H3K9 methyltransferase enzyme, SUV39H1. SUV39H1 trimethylates more H3K9, giving the KRAB repressor the ability to induce reversible repression of transcription at further distances because the chromatin has a stronger DNA:protein interaction (17). Furthermore, HP1α plays a major role in the condensing of chromatin into heterochromatin. Heterochromatin promotes gene silencing because the target genes

are not as easily accessible as before (19). This phenomenon occurs at the transcription start site (TSS), also known as the +1 site.

The overall outcome of dCas9 KRAB recruitment to a specific gene is that the level of that gene, and, therefore, the protein expressed should be reduced, allowing for study of the impact of that gene on cellular function. Because SCCOHT cancer cells may depend on SWI/SNF subunit expression to function, using CRISPRi rather than KO (knock-out) may be a more suitable first approach to investigate exactly how residual SWI/SNF influences the ability of SCCOHT cancer cells to grow and divide.

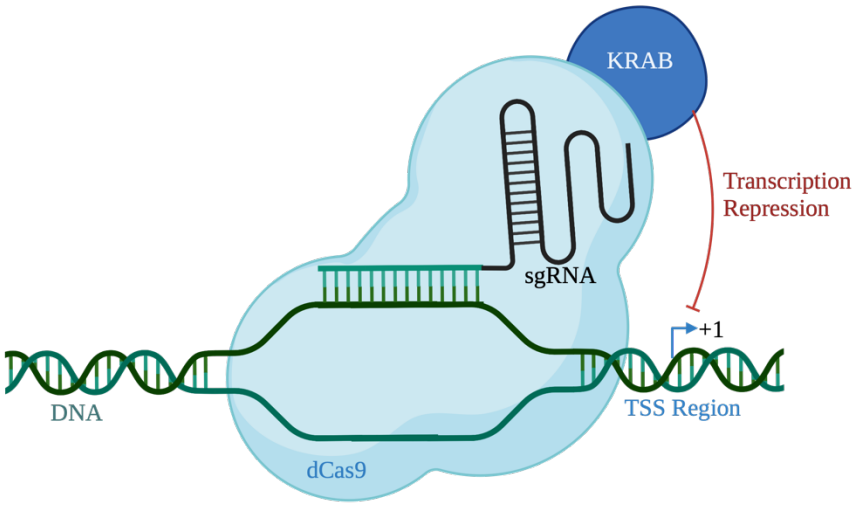

Figure 4. CRISPR Interference (CRISPRi) using a KRAB domain to repress transcription. *The large blue protein represents dCas9 which is bound to the target DNA via sgRNA before the transcription start site region. The dark blue protein represents the KRAB domain which represses transcription by recruiting corepressors to the gene. This Figure was made using BioRender.*

Study Aims and Design

My thesis research involved the interrogation of residual SWI/SNF subunits and their involvement in maintaining SCCOHT cancer function, using genetically engineered SCCOHT cancer cell lines as the model system. Two specific SWI/SNF subunits that have well-studied roles in normal SWI/SNF function are BAF155 and ARID1A. BAF155 is essential for proper assembly of all the mammalian SWI/SNF complexes, which is encoded by the *SMARCC1* gene (20). BAF155 exists as a dimer within all the mammalian SWI/SNF complexes, and without BAF155, the assembly of mammalian SWI/SNF complexes cannot occur (20). In other words, BAF155 is the prerequisite for all SWI/SNF complex formation in cells. ARID1A on the other hand is a subunit that only occurs in cBAF and is essential for the assembly of the ATPase subunit within that complex (21). ARID1A has an extremely important role regarding cBAF in that it ensures that cBAF is recruited to the appropriate areas of the genome (20). Furthermore, ARID1A is a SWI/SNF subunit that is specifically cared about in the ovarian cancer field since more than 40% in all ovarian cancers have an ARID1A mutation (20). The purpose of focusing on these two different subunits for my thesis is that each subunit allows for a different insight to the residual SWI/SNF complex and its role in maintaining SCCOHT cell line function.

Overall, residual SWI/SNF function in SCCOHT is an important aspect to investigate due to the pro-tumorigenic role the complexes seem to have in keeping the cells in a cancer state in previous studies (5, 7, 9, 10, 21). Therefore, if SCCOHT cancer cell lines depend on residual SWI/SNF subunits like has been seen in other cancers marked by

SWI/SNF subunit mutation, I hypothesized that knocking down residual SWI/SNF subunits BAF155 and ARID1A would cause impaired cell proliferation (ability of cells to divide in number), which can be further confirmed through subsequent cell cycle analysis. By focusing on the BAF155 and ARID1A subunits, I can understand the influence of major residual SWI/SNF subunits and their specific effect on keeping SCCOHT cells proliferating. My interrogation of residual SWI/SNF in SCCOHT was done by attempting to knockdown *SMARCC1* and *ARID1A* gene expression levels with the use of cutting-edge technology, CRISPRi, in genetically engineered SCCOHT cell lines (Figure 5). To achieve this outcome, I generated five viral vectors that were used to engineer the COV434 SCCOHT cell line so that it expresses specific CRISPR guide sequences that can target *SMARCC1* and *ARID1A* gene expression. Following engineering of the COV434 cells, I measured knockdown efficiency, cell proliferation, and assessed any cell cycle changes associated with each engineered cell line. The results presented in this thesis allowed me to make some preliminary conclusions not only about residual SWI/SNF function in SCCOHT cells, but also about the use of CRISPRi as a new technique for gene manipulation.

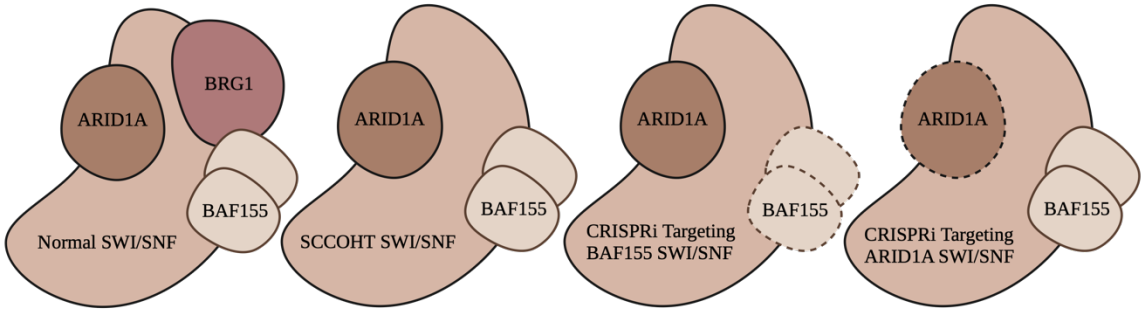

Figure 5. SWI/SNF complexes before and after CRISPRi*. This is a visual representation of the potential SWI/SNF complexes in each of the engineered cell lines generated in this study (the right three complexes) compared to the normal SWI/SNF complex on the left. Decreased BAF155 or ARID1A levels are represented by the dotted lines. This would indicate CRISPRi worked properly, and the cells had decreased expression of the target proteins. This figure was made using BioRender.*

MATERIALS AND METHODS

Viral Vector Generation

The plasmid that was used for the generation of the viral constructs was pXPR_050. pXPR_050 was a gift from John Doench and David Root (*Addgene plasmid # 96925 ; http://n2t.net/addgene:96925 ; RRID:Addgene_96925*). This vector was digested at the BsmB1 restriction site and ran on a 1% agarose gel before being extracted using a gel extraction kit (*Qiagen*). Two guide sequences per gene were chosen using CRISPick with the following parameters: Reference Genome HumanGRCh38 (*NCBI*), Mechanism CRISPRi, and Enzyme SpyoCas9 using Chen 2013 tracrRNA. Oligonucleotides that contain the sgRNA sequences for targeting *SMARCC1* and *ARID1A* were synthesized by Eurofins. The oligonucleotides containing the specific 20 nucleotide guide sequence and BsmBI overhanging bases were annealed into a double stranded

DNA fragment by heating equal amounts together at 95°C and cooling at room temperature. Then the 5' ends of the double stranded DNA template were phosphorylated using PNK (*New England Biolabs*) to allow for insertion into the digested pXPR_050 vector (22). Following ligation of the insert with the vector, the ligation products were transformed into XL1BLUE competent cells and plated onto LB/agar plates containing ampicillin. Multiple bacterial colonies from each transformation were screened by using a primer that anneals within the U6 promoter. Sanger sequencing was performed by Molecular Cloning Laboratories. Once verified, a fresh transformation was performed using the validated plasmid DNA, which then was used to archive the construct in a glycerol stock stored in -80°C and generate a large amount of plasmid DNA through a maxi-prep protocol (*Invitrogen*).

Cell Culture and Cell Line Engineering

BIN67 and COV434 cell lines were a kind gift from Bernard Weissman at UNC Chapel Hill. dCas9 KRAB expressing BIN67 and COV434 cells were engineered before I began my portion of the project. HEK239T cells used to create viral particles and are made using Weissmiller lab stocks. BIN67, COV434, and all engineered derivatives are maintained in RPMI-1640 media with l-glutamine containing 10% Fetal Bovine Serum (FBS) and 1% Penicillin/Streptomycin (P/S). DMEM with 10% FBS and 1% P/S is the maintenance media used to maintain the HEK293T cells. All cells were maintained in an incubator held at 37^{o}C with 5% carbon dioxide. SCCOHT cell lines were engineered through viral transductions. Viral particles were generated by transfecting HEK293T cells with the appropriate pXPR_050 vector, the Pax2 packaging vector, and the pMD2

envelope vector using calcium phosphate transfection method. Viral particles in the supernatant were collected in SCCOHT cell line maintenance media over a three-day period and placed in cryovials to be stored in -80°C until use. To begin cell line engineering, one million dCas9 KRAB-expressing cells were plated in 60 mm tissue culture dishes. The day after plating, the respective viral supernatant was placed on the cells to allow for transduction. Transduction occurred for all cells over two days using fresh viral supernatant each day and then all cells were allowed to recover for one day without virus. To select for engineered cells in the population, 1 μg/ml puromycin was added in maintenance media. After three days with the antibiotic maintenance media the cells were observed to see if how the transduced cells were compared to a selection control to ensure transduction success, and then all cells allowed to recover in regular maintenance media. This process occurred to produce the following cell lines, using the dCas9 KRAB SCCOHT line as the parental cell: *SMARCC1* Guide 1, *SMARCC1* Guide 2, *ARID1A* Guide 1, *ARID1A* Guide 2, and empty vector control (pXPR_050). An empty vector control cell line was generated independently for each portion of the study shown in the results section.

Cell Proliferation and Cell Cycle Analysis

5.0 x 10^5 engineered COV434 cells were plated onto separate plates and allowed to grow for three days. The number of cells on the plates were counted by using the ThermoFisher Countess II and trypan blue stain. Following calculation of total cell numbers, one million cells from the population were collected for the cell cycle analysis by centrifugation and fixation in ice-cold 70% ethanol and storage in -20°C overnight. To

prepare for cell staining, the cells were removed from the freezer and allowed to thaw at room temperature prior to centrifuging cells at 800 x g for 6 minutes. Cells were then washed in 1X phosphate buffered saline (PBS) and centrifuged again at 800 x g for 6 minutes. Finally cells were resuspended in propidium iodide (PI) staining solution (containing 1X PBS, 10 μg/ml propidium Iodide (PI), 100 μg/ml RNAse A, 2 nM $MgCl_2$) and allowed to sit overnight at 4°C. Stained cells were then filtered using a 35 μm nylon mesh cell strainer and a minimum of ten thousand stained cells were recorded for each cell line using a Guava easyCyte flow cytometer (*Luminex*) with selection for single cells based on forward and side scatter. Three biological replicates were performed for statistical comparison with all information located in the figure legend.

Protein Lysates

Maintenance media from cultured cells was aspirated before washing the cells twice with a 1X PBS solution. The cells were then scraped, and the cell suspension was collected in a 1.5 ml tube. The cells were pelleted using a tabletop centrifuge set to 13,000 RPM for two minutes. Cell pellets were resuspended in 250 μL of freshly made lysis buffer containing 0.1 M PMSF (*Tocris Bioscience*), protease inhibitor cocktail (*Roche*), and 1% Triton X-100, 150 mM NaCl, 5 mM EDTA, and 50 mM Tris, pH 8.0 and lysed via sonication on 25% power for 15 seconds. The debris was spun out through centrifugation at 13,000 RPM for 10 minutes in a centrifuge held at 4°C. The samples were normalized to each other using the BioRad protein assay dye and bovine serum albumin to generate a standard curve. Once normalized, a loading dye containing sodium dodecyl sulfate (SDS) and β-mercaptoethanol (BME) was added to each tube as well as

lysis buffer before being boiled at 95°C for 5 minutes. These protein lysates were stored at -20°C until used in Western blots.

Western Blotting

Protein lysates that were previously prepared and stored at -20°C were thawed on ice, and 10-30 μg was loaded into the correct percent SDS page gel. Once the apparatus was placed together which contained the gel, 1X Tris-glycine running buffer (50 ml 10X Tris-glycine running buffer [30.3 g Tris Base, 144 g Glycine, 10 g SDS, fill to 1 L with MilliQ 18 Ohm water] and 450 ml MilliQ 18 Ohm water), and electrophoresis components, the proteins were stacked at an even level for 10 minutes at 100 volts. After the stack, the gel was run for an hour at 130 volts. A sandwich containing sponges, filter paper, PVDF membrane, the SDS-PAGE gel, filter paper, and sponge in a cassette was formed and placed in an electrophoresis chamber with an icepack in 1X transfer buffer (100 ml methanol, 800 ml MilliQ 18 Ohm water, and 100 ml 10X transfer buffer [30.3 g Tris Base, 144 g Glycine, fill to 1 L with MilliQ 18 Ohm water]). The transfer occurred at an hour and 10 minutes at 100 volts. The PVDF membrane with freshly transferred proteins was then cut for corresponding primary antibodies to probe the membrane. Fresh 5% block was made (2.5 grams of dry milk powder and 50 ml of TBS-T), and the PVDF membranes were soaked in the block solution on a shaker plate for an hour at room temperature. This block solution was then discarded. Primary antibodies of interest were thawed on ice before being diluted in block buffer at the correct ratio. These antibodies remained on the PVDF membrane overnight in a refrigerated room on a shaker plate. Tris-buffered saline containing 0.1% Tween-20 (TBS-T) was used to wash the blot three

times for five minutes each (discarded in between each repetition). Secondary antibody was thawed on ice before being diluted with block at the correct ratio and placed on the respective PVDF membrane sections. TBS-T was used to wash the blot three times for five minutes each (discarded in between each repetition). The protein bands were developed by the normal or maximum (when necessary) Clarity ECL substrate (*BioRad*), and visualized on a BioRad ChemiDoc MP instrument. The antibodies used for this research are as follows: ARID1A (*Cell Signaling*, 12354S), BRG1 (*Cell Signaling*, 49360S), PBRM (*Cell Signaling*, 89123S), BAF155 (*Cell Signaling*, 11956S), BRD7 (*Cell Signaling*, 15125S), GAPDH-HRP (*Cell Signaling*, 8884S), Cas9 (*Cell Signaling*, 14697T).

mRNA Analysis and QPCR

To extract RNA, cells were pelleted at 13,000 RPM for two minutes in a centrifuge. The pellet was resuspended thoroughly in 600 µl of Trizol before being vortexed. The sample then was rotated at room temperature for 20 minutes. All RNA was extracted using the Zymo direct-zol RNA Miniprep kit. Synthesis of cDNA from the RNA in each sample was completed via the Promega M-MLV Reaction. This process uses the Reverse Transcriptase enzyme, so control samples were run concurrently. The thermal cycler used for this reaction was the BioRad S1000. To run qPCR, nuclease-free water, the cDNA, master mix (Perfecta SYBR), and corresponding primers (5µM of each forward and reverse) were pipetted onto a 96 well plate. The primer sequences used targeted specific areas of the *SMARCC1* and *ARID1A* gene and primers against a housekeeping gene (GAPDH) were used for normalization. An empty vector samples as

well as parental control were included determining mRNA knockdown. All graphs were generated using Prism GraphPad Software.

RESULTS

First, I validated the BIN67 and COV434 SCCOHT cell lines obtained from a collaborator for absence of the BRG1 subunit by performing a SWI/SNF panel using Western blot analysis (Figure 6A). There were six cell lines included that derived from various types of cancers including MRT (SNF5-null), SCCOHT (BRG1-null), and neuroblastoma (normal SWI/SNF subunit expression). These cell lines were chosen based on their different SWI/SNF subunit expression and used for comparisons. This figure validates that both BIN67 and COV434 cell lines lacked BRG1 expression as expected. The BIN67 and COV434 cells were then engineered to express dCas9 KRAB through viral transduction which was validated by performing a Western blot to probe Cas9 levels in the engineered cells versus the parental cells (Figure 6B). Following validation of Cas9 expression, the dCas9 KRAB BIN67 and COV434 cells were then used for subsequent engineering to perform CRISPRi knockdown of specific SWI/SNF subunits.

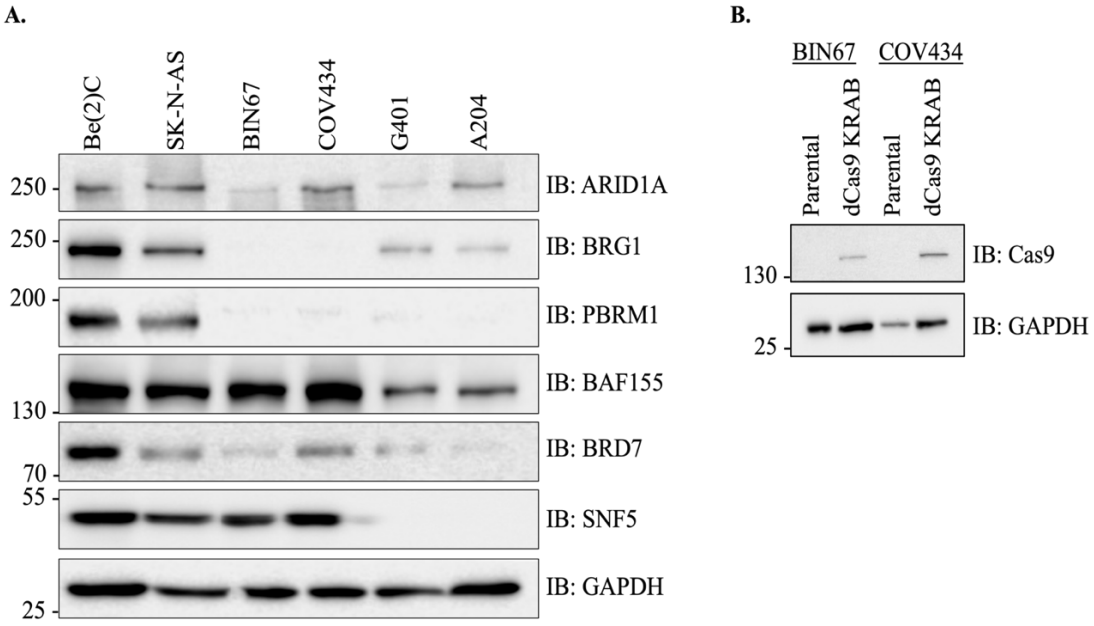

Figure 6. Validation of cell lines used in the project. *Validation of BIN67 and COV434 for absence of BRG1. (A) This figure is a Western blot panel for BAF subunits to validate the SCCOHT cell lines BIN67 and COV434 that the laboratory received. ARID1A is mutually exclusive to the cBAF complex BRG1 and BAF155 are present in all BAF complexes. PBRM1 and BRD7 are mutually exclusive to the pBAF complex. SNF5 is present in cBAF and pBAF only. Be(2)C and SK-N-AS are neuroblastoma cell lines that have expression of all tested subunits and serve as a control for expression. G401 and A204 are MRT cell lines that are known to be SNF5 null. (B) Validation of dCas9 KRAB BIN67 and dCas9 KRAB COV434 for expression of Cas9. These cell lines became the parental cell line for expression of guide RNAs in the remaining experiments. All Western blots were imaged using BioRad ImageLab Software.*

To complete the CRISPRi process, the dCas9 KRAB BIN67 and COV434 cell lines (referred to as my parental cell lines in remaining figures) also needed to be engineered to express a sgRNA, which would work to target dCas9 KRAB to the proper gene target. To target dCas9 KRAB to *SMARCC1* or *ARID1A* genes, I generated viral vector constructs containing unique 20 nucleotide guide sequences for *SMARCC1* and *ARID1A* targets. The guide sequences were chosen using the CRISPick tool that chooses the top guides for *SMARCC1* and *ARID1A* while minimizing off-target effects and maximizing on-target effects. For this, the plasmid that was used to generate the viral constructs was pXPR_050, which is shown below in Figure 7 with the restriction enzyme

sites for BsmBI annotated. At these BsmBI sites, I was able to insert each specific guide sequence through molecular cloning techniques as described in the materials and methods.

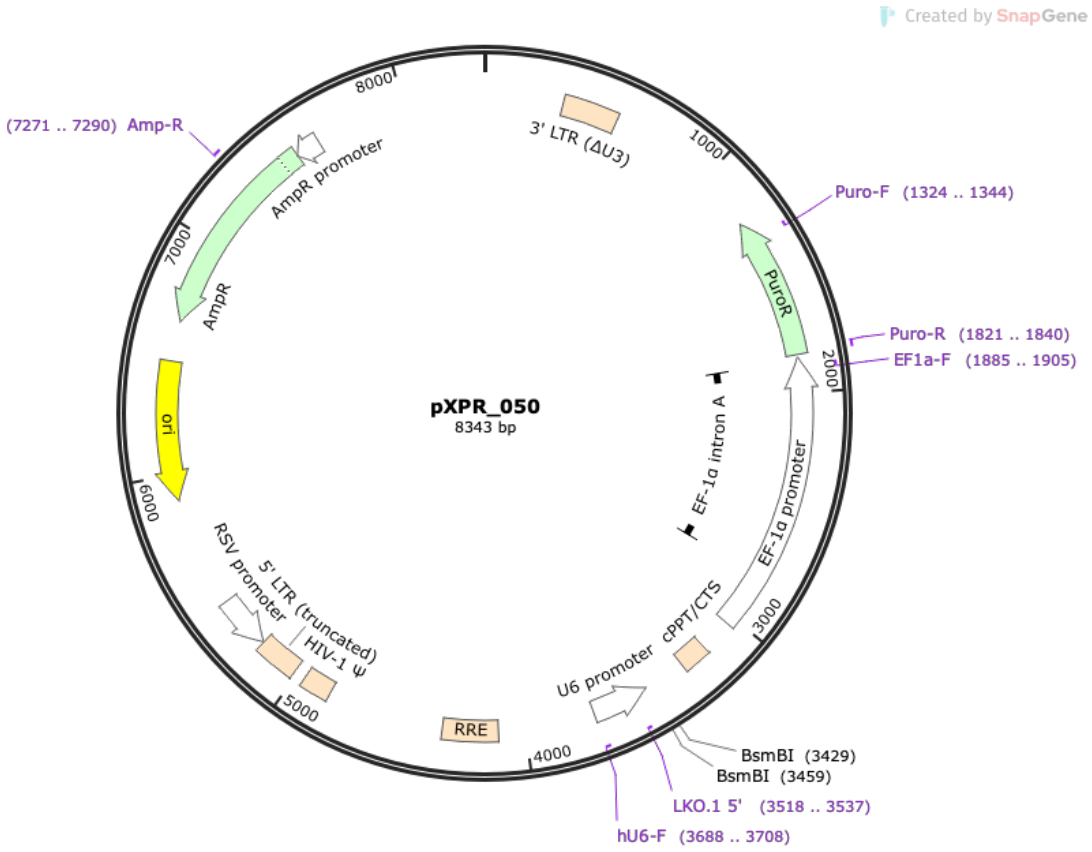

Figure 7. Plasmid map of pXPR_050. *The pXPR_050 plasmid was cut at the BsmBI restriction site to insert guide sequences necessary for CRISPRi. This plasmid containing no guide sequence was used as the pXPR_050 empty vector control for the knockdown experiments to follow. Plasmid map created using SnapGene software.*

For each target, I chose two separate guide sequences from CRISPick, making a total of four viral vectors that I generated which would be used in comparison to the empty pXPR_050 vector to determine knockdown efficiency (Figure 8A). All pXPR_050 guide vectors were validated through Sanger sequencing analysis. The Sanger sequencing results for the region surrounding the inserted 20 nucleotide guide sequence for each

construct I generated are shown in Figure 8B. These results validate that the engineered viral vector constructs contain the guide sequences necessary to complete cell line engineering for CRISPRi to target *SMARCC1* and *ARID1A* target genes in SCCOHT cell lines.

A.

Viral Vector	Inserted Guide Sequence	Intended Use
pXPR_050	Empty Vector Control	Normal Protein Expression
pXPR_050	GGGTGCGCGCGGGAACGACC	SMARCC1 Guide 1 (Pick 2)
pXPR_050	AACGACCGGGAAACACCGCG	SMARCC1 Guide 2 (Pick 4)
pXPR_050	GAAAGCGGAGAGTCACAGCG	ARID1A Guide 1 (Pick 1)
pXPR_050	AGAAAGCGGAGAGTCACAGC	ARID1A Guide 2 (Pick 3)

B.

ARID1A Guide 1

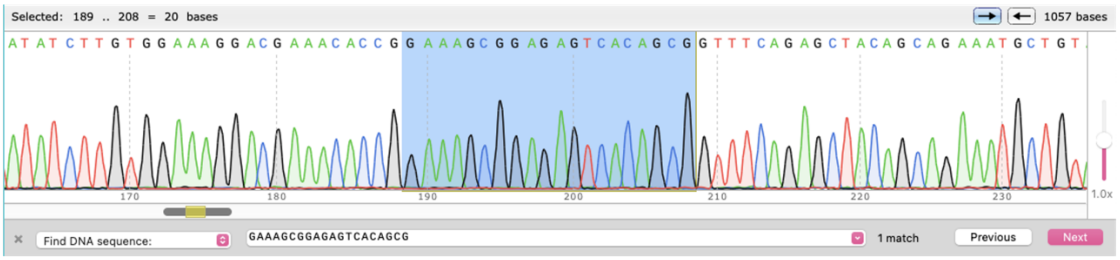

ARID1A Guide 2

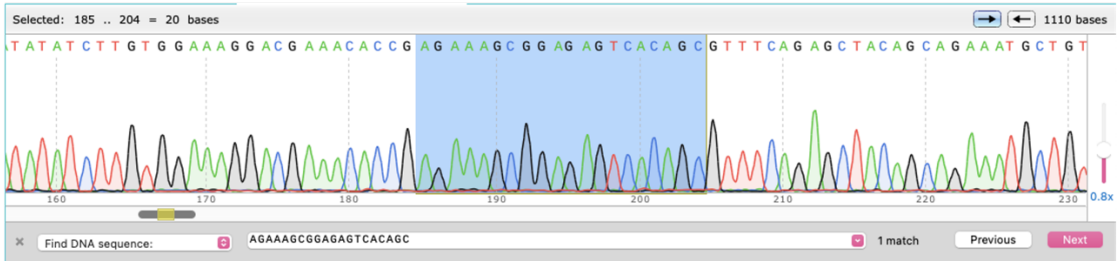

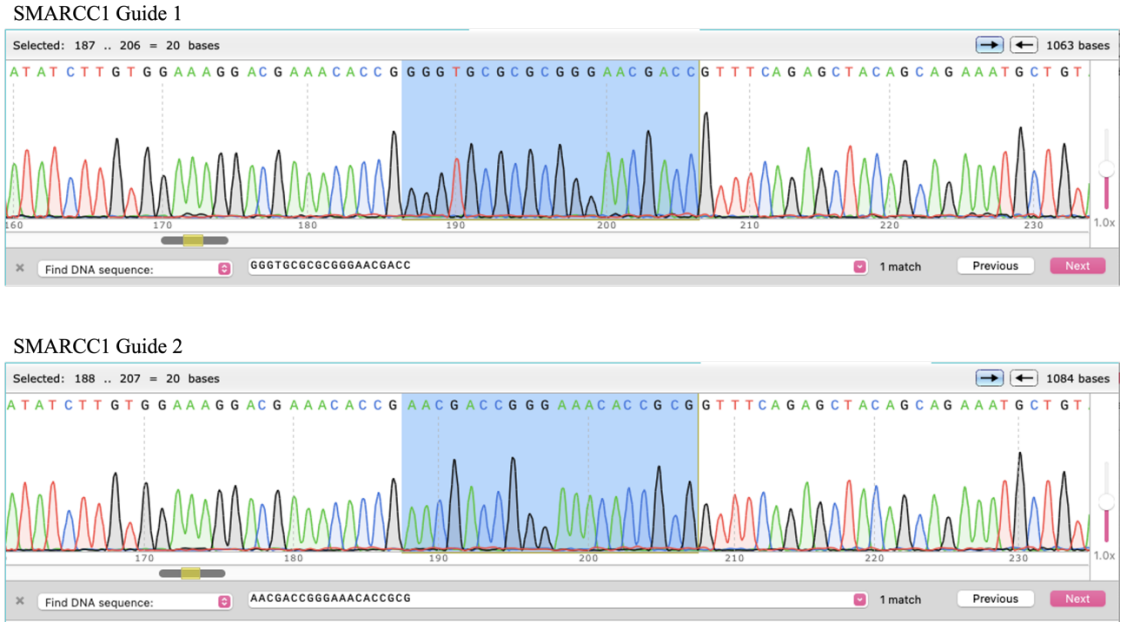

Figure 8. Generation and validation of viral constructs to be used for CRISPRi. *(A) The pXPR_050 transfer plasmid was used as a backbone viral vector for insertion of guide sequences to target the ARID1A and SMARCC1 (BAF155) gene. Guide sequences were selected using the CRISPick program and are listed here, along with their intended use in the project. (B) Insertion of the guide sequences into pXPR_050 was confirmed using Sanger sequencing technology. Sequence chromatograms of the region surrounding the insertion site is shown for both SMARCC1 and ARID1A and the 20 nucleotide guide sequence highlighted.*

dCas9 KRAB-expressing BIN67 and COV434 parental cells were used to express the sgRNA sequences through viral transduction. Successful integration of the guide sequences into the SCCOHT genome through viral transduction could be confirmed by antibiotic selection in puromycin. This is because the puromycin resistance gene was also included as a coding sequence that would be integrated into the genome during the transduction process. The first set of transductions attempted were completed using the parental dCas9 KRAB BIN67 cell line with the *SMARCC1* guide sequences. However, these cells did not survive the selection phase with puromycin. Attempts to optimize puromycin selection of BIN67 cells were repeated several times, however, this cell line

showed to be difficult to complete engineering on. Therefore, COV434 cells were chosen as the example SCCOHT cell line for completion of this project.

There are several advantages I observed about COV434 cells when working with them that make these cells ideal for this project. First, these cells are easier to maintain in cell culture as they are smaller and have a high doubling time of 24.9 hours. In addition, the BIN67 cells tend to cluster together which make it difficult to get individual cells for the applications I would do such as flow cytometry, but COV434 cells did not have this characteristic. This makes them more amenable to the experiments I planned. Since there are only three SCCOHT cell lines that have been derived from this rare cancer, continuing with COV434 was an optimal starting point for residual SWI/SNF subunit interrogation.

Therefore, dCas9 KRAB COV434 cells were first engineered to express guides targeting ARID1A with inclusion of engineering a cell line to express the empty pXPR_050 vector control. Following selection in puromycin, the cells were allowed to recover and then were used for a variety of assays including mRNA analysis, protein analysis, cell proliferation, and cell cycle assays. Examination of mRNA levels of *ARID1A* expression revealed that compared to the empty vector pXPR_050 transduced COV434 cell line there is minimal (~20%) level of knockdown (Figure 9A). Western blot analysis at this same time point was also performed. The Western blot showed no detectable knockdown of ARID1A protein levels compared to the control samples (Figure 9B). Consistent with little to no knockdown of *ARID1A*, there was no change in cell proliferation compared to the parental dCas9 KRAB COV434 cell line (Figure 10A,

B). Regardless, I completed cell cycle analysis to master this technique for my thesis work since it is a technically demanding technique. Cell cycle analysis was completed using flow cytometry methods and the gating strategy I used for these samples is shown in Figure 10C. Again, consistent with all other assays, there is no significant differences in the cell cycle histograms compared to the empty vector control (Figure 10D, E). Taken together, the lack of sufficient knockdown at both the mRNA and protein levels at the time of these experiments prevents me from concluding how ARID1A impacts the ability of SCCOHT cells to grow and divide.

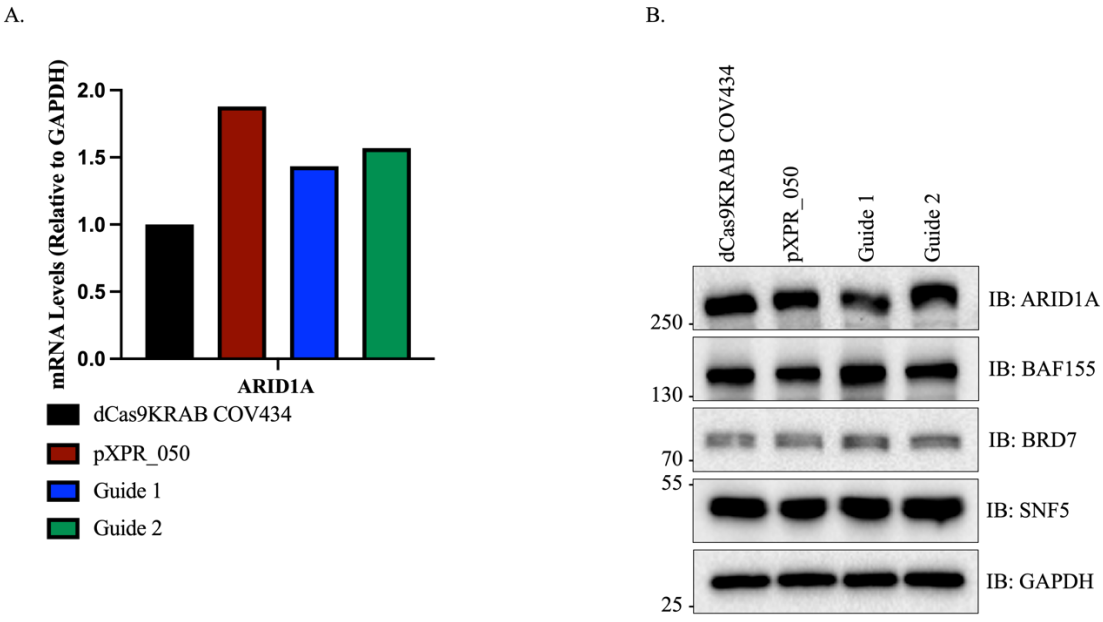

Figure 9. Impact of CRISPRi on ARID1A mRNA and protein levels. *(A) RNA was extracted from COV434 cell lines expressing either guide 1 or guide 2 targeting ARID1A for knockdown, or no guide (pXPR_050) following puromycin selection. One ARID1A primer that targets ARID1A was used for qPCR to measure the amount of ARID1A mRNA levels. CRISPRi knockdown of the ARID1A gene showed reduced expression at the transcript level of around 20% compared to the cells expressing the empty vector. The cell lines expressing the empty vector pXPR_050 do not express comparable levels of ARID1A to the COV434 dCas9 KRAB parental cell lines. (B) Western blot analysis was performed on proteins extracted from indicated cell lines. ARID1A protein levels were not reduced in cell lines expressing guide 1 and guide 2 and other BAF subunits probed show similar levels. GAPDH is also included as a loading control.*

A.

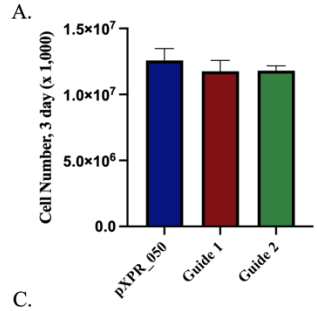

B.

Cell Line	Replicate 1 [Total Cell #]	Replicate 2 [Total Cell #]	Replicate 3 [Total Cell #]
dCas9 KRAB COV434 pXPR_050 for *ARID1A*	13,700,000	13,250,000	10,800,000
dCas9 KRAB COV434 A1	12,350,000	12,800,000	10,100,000
dCas9 KRAB COV434 A2	11,100,000	11,950,000	12,350,000

C.

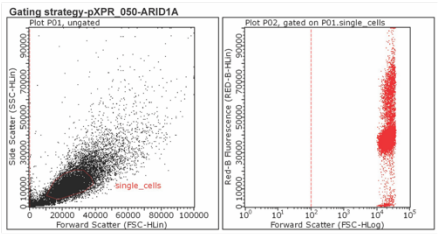

D.

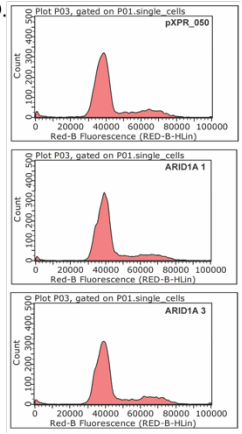

E.

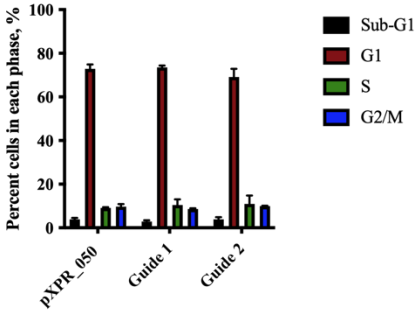

Figure 10. Effect of CRISPRi on cell proliferation and cell cycle phase distribution. *(A, B) Indicated engineered cell lines were plated in equal amounts and then allowed to proliferate for three days. Cell numbers were then determined on day three and total cell numbers on this day were graphed for each sample. Cells expressing both guide 1 and guide 2 show no significant change in cell proliferation (n=3 biological replicates, error bars are standard error of the mean, using unpaired t-test, two tailed). (D) Cell cycle phase distribution analysis was performed as a secondary approach for each engineered cell line. Image shows the quality of flow cytometry data obtained and the gating strategy to select single cells with propidium iodide signal. (D) Representative images show the cell cycle profile of the dCas9 KRAB COV434 pXPR_050, ARID1A guide 1, ARID1A guide 2 cell lines. (E) Each cell cycle phase was quantified across all replicates and then graphed (n=3 biological replicates, error bars are standard error of the mean, using unpaired t-test, two tailed). The graphs were generated on Prism Graphpad Software and flow cytometry data obtained using InCyte Software.*

dCas9 KRAB COV434 cells were engineered next to express guides targeting *SMARCC1* (BAF155 protein) or an empty pXPR_050 vector control. mRNA analysis using two different primer sets showed that *SMARCC1* is knocked down to around 50% levels when compared to the empty vector and parental controls (Figure 11A). A Western blot panel showed comparable levels of knockdown for the BAF155 protein, as well as for other SWI/SNF subunit members such as BRD7 and SNF5 (Figure 11B). This indicates that decreasing BAF155 is sufficient to impact levels of many SWI/SNF

subunits which is consistent with its identification as a core SWI/SNF protein. Interestingly, cell proliferation results showed that dCas9 KRAB guide expressing COV434 cells tended to have increased proliferation compared to the empty vector control COV434 cell line (Figure 12A, B) with guide 2 causing a significant increase in cell number. Subsequent cell cycle analysis was completed using flow cytometry and the gating strategy used is shown in Figure 12C. Quantification of cell cycle phase distribution for all samples revealed one significant difference seen in the G2/M phase between the guide 2 and empty vector control expressing cell lines (Figure 12D, E). Thus, this suggests the expression of this guide promotes more cells to be present in this phase and it is consistent with an increase in cell proliferation (Figure 12A). These data combined with the cell proliferation data indicate that rather than knockdown of BAF155 reducing SCCOHT cell growth and division as I hypothesized, the reduction in BAF155 levels instead leads to a modest pro-growth phenotype that either was significant (guide 2) or trended in that direction (guide 1).

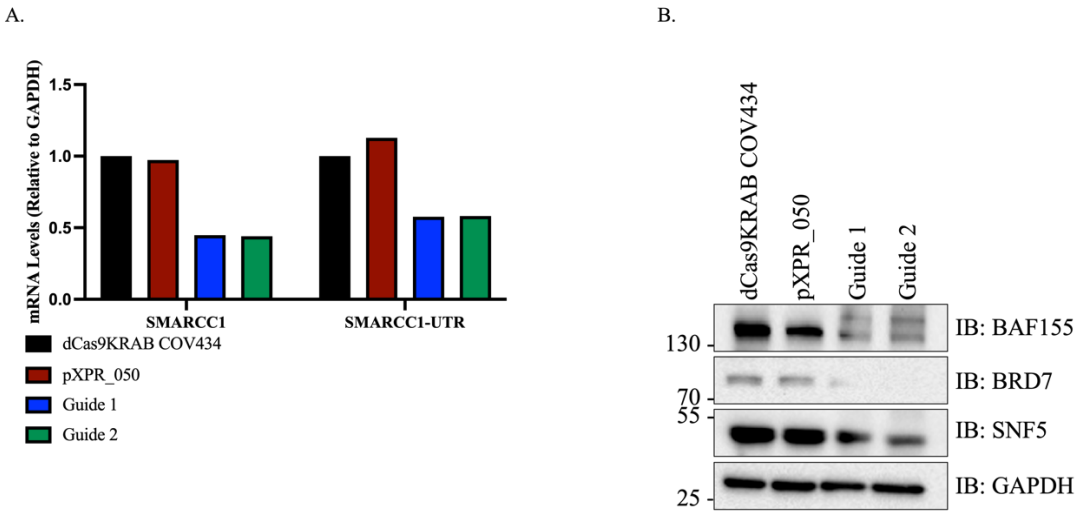

Figure 11. Knockdown of SMARCC1 at the mRNA and protein level. *(A) RNA was extracted from COV434 cell lines expressing either guide 1 or guide 2 targeting SMARCC1 for knockdown, or no guide (pXPR_050). Two different SMARCC1 primers that target different regions of SMARCC1 were used for qPCR to measure the amount of SMARCC1 mRNA levels. "UTR" is the "3' untranslated region." CRISPRi knockdown of the SMARCC1 gene showed reduced expression at the transcript level of around 50%. The cell lines expressing the empty vector pXPR_050 express comparable levels of SMARCC1 to the COV434 dCas9 KRAB parental cell lines. (B) Western blot analysis was performed on proteins extracted from indicated cell lines following puromycin selection. BAF155 (SMARCC1) protein levels were reduced in cell lines expressing guide 1 and guide 2 and other BAF subunits probed show similar levels of knockdown. GAPDH is also included as a loading control.*

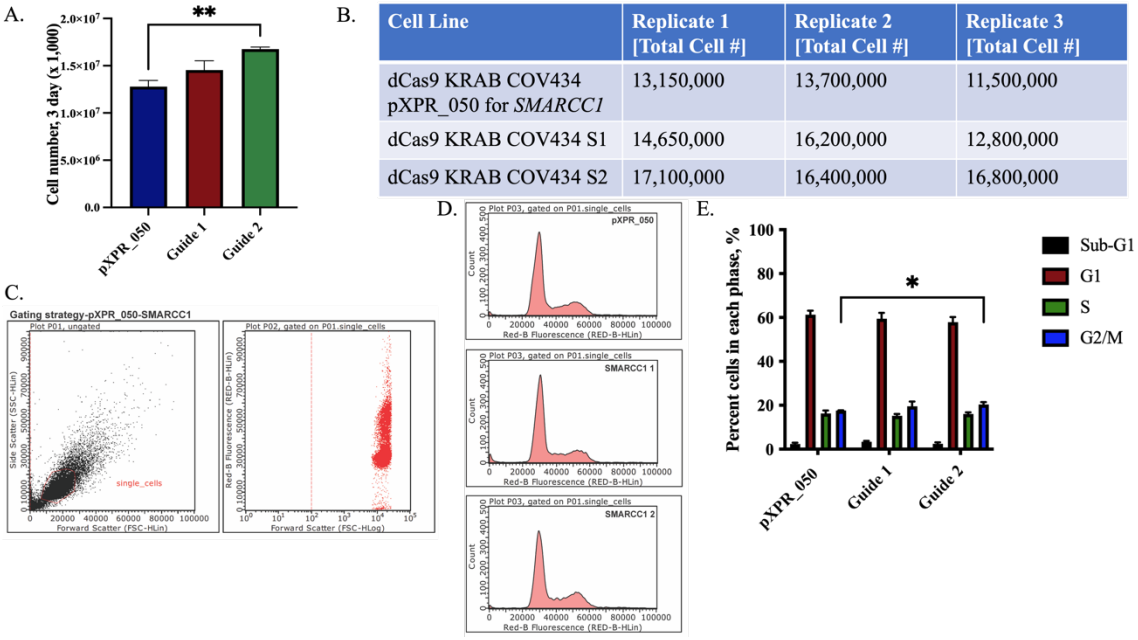

Cell Line	Replicate 1 [Total Cell #]	Replicate 2 [Total Cell #]	Replicate 3 [Total Cell #]
dCas9 KRAB COV434 pXPR_050 for *SMARCC1*	13,150,000	13,700,000	11,500,000
dCas9 KRAB COV434 S1	14,650,000	16,200,000	12,800,000
dCas9 KRAB COV434 S2	17,100,000	16,400,000	16,800,000

Figure 12. Effect of SMARCC1 knockdown on cell proliferation and cell cycle phase distribution. *(A, B) Indicated engineered cell lines were plated in equal amounts and then allowed to proliferate for three days. Cell numbers were then determined on day three and total cell numbers on this day were graphed for each sample. Cells expressing guide 2 show a significant change in cell proliferation, while expression of guide 1 trends in a similar direction (n=3 biological replicates, error bars are standard error of the mean, *P= 0.0045 using unpaired t-test, two tailed). (D) Cell cycle phase distribution analysis was performed as a secondary approach for each engineered cell line. The image shows the quality of flow cytometry data obtained and the gating strategy to select single cells with propidium iodide signal. (D) Representative images show the cell cycle profile of the dCas9 KRAB COV434 pXPR_050, SMARCC1 guide 1, SMARCC1 guide 2 cell line (E) Each cell cycle phase was quantified across all replicates and then graphed (n=3 biological replicates, error bars are standard error of the mean, *P= 0.0150 using unpaired t-test, two tailed). A modest increase of cells in the G2/M phase of cell cycle was present for the dCas9 KRAB COV434 SMARCC1 guide 2 cell line. The graphs were generated on Prism Graphpad Software and flow cytometry data obtained using InCyte Software.*

In addition to interrogation of residual SWI/SNF function in SCCOHT cells, part of my thesis work was to bring a new technique like CRISPRi into the laboratory. Therefore, I spent some time assessing how knockdown of these subunits changed over the course of time in cell culture. Variation in gene knockdown across a population can occur due to a variety of factors, including unequal expression of gene products within

the cell population or cell drift that occurs as cells respond to knockdown of targets (23). Therefore, I allowed engineered cell lines to grow in culture for an extended period, which was close to one month and then collected all cell lines for Western blot analysis of both ARID1A and BAF155 knockdown in dCas9 KRAB COV434 cell lines. Surprisingly, knockdown of ARID1A appeared to get stronger over time as seen in Figure 13A compared to Figure 9. However, the BAF155 knockdown was absent for both guide sequence cell lines shown in Figure 13B compared to Figure 11 where knockdown was apparent. There could be many possibilities as to why this phenomenon occurred, so to dive deeper into the creation of this phenomenon we decided to run a Cas9 blot to see if levels of dCas9 KRAB expression in the population of cells correlate with changes in knockdown efficiency. Results show that the Cas9 protein levels increase over time in the *ARID1A*-guide expressing cell lines (Figure 14A) while the Cas9 protein levels decrease over time in the *SMARCC1*-guide expressing cell lines (14B), indicating that the level of dCas9 KRAB expression in the population correlates with the level of CRISPRi-mediated knockdown of *ARID1A* and *SMARCC1*. This suggests that variation with the level of Cas9 within the population, through cell drift or other cellular processes, can dictate the level of knockdown within the population of study using CRISPRi. Future experiments aimed at examining clonal versions of cells that express consistent levels of dCas9 may be able to provide future insight into issues with cells drifting in knockdown efficiency.

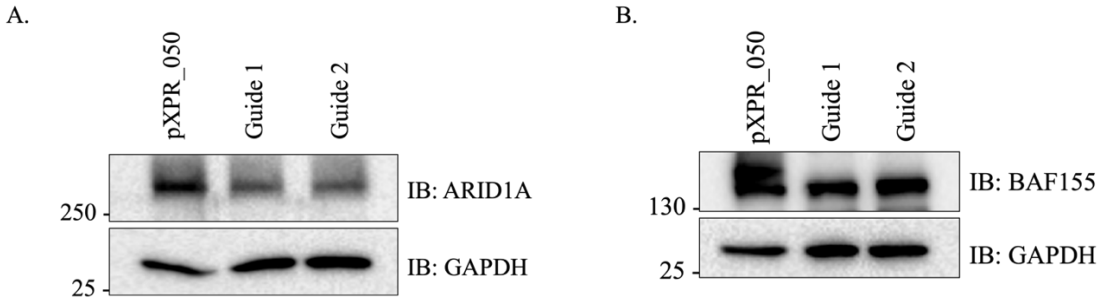

Figure 13. Long term effect of CRISPRi knockdown of ARID1A and SMARCC1. *(A) Western blot analysis was performed on proteins extracted from indicated cell lines after approximately one month following puromycin selection. ARID1A protein levels are reduced compared to those expressed in the pXPR_050 cell line. (B) Analysis as in (A), except for SMARCC1 engineered cell lines. BAF155 (SMARCC1) protein levels are similar to those expressed in the pXPR_050 cell line.*

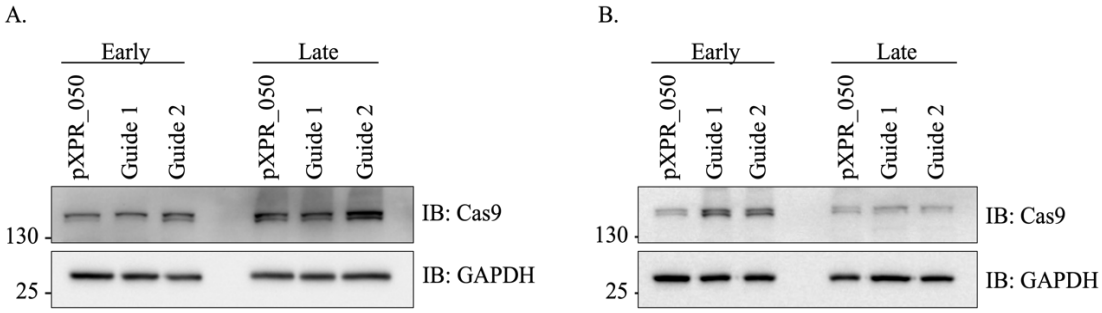

Figure 14. Analysis of Cas9 protein levels in engineered cell lines during the engineering process. *Western blot analysis was performed on proteins extracted from indicated cell lines following puromycin selection (early) and approximately one month after puromycin selection (late). (A) The Cas9 protein levels in the ARID1A engineered cell lines moderately increases and correlates with enhanced knockdown effect observed in Figure 13A. (B) The Cas9 protein levels in the SMARCC1 engineered cell lines decreases as cells continue to proliferate and correlates with reduced knockdown effect observed in Figure 13B.*

DISCUSSION

Understanding the mechanisms of dual ATPase loss on SCCOHT cell lines will be critical for finding new therapy options for patients. The tissue of origin of SCCOHT cells remains unknown (2) which further complicates treatments for patients with this cancer because there is not a specific type of chemotherapy to use. Thus, this project was intended to identify possible essential subunits to target in the residual SWI/SNF complex. The original hypothesis for this project was if SCCOHT cell lines depend on either residual SWI/SNF subunit, BAF155 or ARID1A, then knockdown of either may impair cell proliferation which could be confirmed through cell cycle analysis. However, the results observed in the case of BAF155 knockdown did not support the hypothesis as there was not a negative impact on cell proliferation (Figure 12A, B). A surprising result that was seen with the *SMARCC1* guide 2 knockdown was a pro-growth phenotype in both the cell proliferation and cell cycle analyses (Figure 12) and a trend in increased cell proliferation was seen using guide 1 as well. There was a significant increase with guide 2 consistently between both assays and specifically, there was a higher number of cells seen in the G2/M phase meaning these cells were entering/currently in the mitosis phase of the cell cycle which ends with cell division (Figure 12E). There is an expectation that any phenotype measured should correlate with the level of knockdown and in the case of BAF155, both guides caused reduction of BAF155 to the same level (Figure 11). Therefore, because cell proliferation and cell cycle phase distribution are not significantly increased with both guides it may be that this phenotype is not directly due to decreased BAF155 levels and is some artifact of cell line engineering. On the other hand, if the tendency for knockdown of BAF155 to lead to a trend in cancer cell division, this may be

an indication that residual SWI/SNF could retain tumor suppressive abilities rather than pro-tumorigenic abilities as has been seen in other SWI/SNF-altered cancers. In other words, the other subunits present in the residual SWI/SNF complex still confer some function in inhibiting or slowing cell division just like normal SWI/SNF complexes are thought to do. Future experiments will be needed to differentiate these two possibilities.

Beyond probing the contribution of SWI/SNF subunits in SCCOHT, part of my research was to provide a solid foundation for using CRISPRi since it was a new technique to the laboratory. A difficulty when using knockdown approaches or populations of cells undergoing perturbations is cell drift, which is when cells within a population have differences in growth rates or other characteristics. If not all cells in a population are responding the same, or engineered to the same degree, then it is possible for some cells to have a selective advantage in growth within the population causing a selection for a specific phenotype to occur. For this project, COV434 SCCOHT cells were engineered to express dCas9 KRAB, so the cell line would be able to undergo CRISPRi mechanisms. However, it is likely that not all the cells in the population were expressing the same levels of Cas9 which may contribute, as my data suggests (Figure 14) to the efficiency of knockdown. In a mixed population, some cells may experience more or less CRISPRi-mediated knockdown of the target and in response to that perturbation the cells may have more or less growth, leading to cell drift and difficulty maintaining consistent knockdown levels. For example, if the cells in the population selected for lower expression of Cas9 (Figure 14B), then the knockdown of protein, BAF155, would also be low and not remain for an extended period of time (Figure 11B compared to Figure 13B). For future CRISPRi projects, I would propose that the first step

would be to clone out the engineered dCas9 KRAB cells to identify which clones have the highest expression of Cas9 and engineer that specific clonal cell line. This would prevent cell drift and give a very low chance of the knockdown varying because there would be equal expression of Cas9 amongst all cells, so theoretically all cells should have the same level of knockdown. Thus, the growth levels associated with expression of Cas9 and the cell's ability to undergo CRISPRi processes would be similar, and it would be extremely difficult for the cells to drift. While CRISPRi is a very new field, these types of issues are known to occur with shRNA knockdown approaches. The process of cloning out cell lines for CRISPRi has been done with multiple common engineered cell lines, such as HEK293T and HeLa cells, to minimize phenotypic variability while using CRISPR systems (23). Another possible route would be to use CRISPR knockout of essential genes, which may be more suitable for this specific circumstance using SCCOHT cells since my data indicate that knockdown of BAF155 is not essential to cell survival.

At this time, the results gathered from the ARID1A portion of this project are uninformative due to the knockdown not being present early after engineering. However, the knockdown of ARID1A became more prominent over time as the cells grew out in cell culture (Figure 9B compared to Figure 13A). Again, due to cell drift issues, there needs to be further optimization with the engineering of the dCas9 KRAB parental cell lines before future ARID1A studies are completed. On the other hand, slight knockdown was achieved with both CRISPRi guides, so the guide sequences chosen do indeed work. The CRISPRi system is new to the genetics field with limited publication using it currently but has been successfully used to observe both essential and non-essential genes

in species such as *L. plantarum* (24). Myrbraten *et al.*, however, did record a correlation that the sgRNAs did have off-target effects in cells with higher levels of Cas9 expression. According to Fu *et al.* (25), when off-target effects are occurring, there is a higher chance for phenotypic variability amongst cells for the same target gene. Thus, this could be another factor for some cells in the population obtaining a better knockdown than others. CRISPRi typically should not have off-target effects due to the specificity of the sgRNAs, but it is not something that can be eliminated entirely. This is why it is crucial to pick guide sequences with minimal off-target effects and maximum on-target effects when engineering constructs as I attempted in this study.

In closing, the use of CRISPRi systems on residual SWI/SNF subunits is an auspicious route to uncover essential genes to target as novel therapy options for SCCOHT cancer. My thesis work set a foundation for future studies not only using this technique effectively but in interrogating synthetic lethal targets in this deadly young adult cancer.

WORKS CITED

(1) Estel R., Hackethal A., Kalder M., Munstedt K. Small cell carcinoma of the ovary of the hypercalcemic type: an analysis of clinical and prognostic aspects of a rare disease on the basis of cases published in the literature. Arch Gynecol Obstet. 2011;284(5):1277-82.

(2)Young R.H., Oliva E., Scully R.E. Small cell carcinoma of the ovary, hypercalcemic type. A clinicopathological analysis of 150 cases. Am J Surg Pathol. 1994;18(11):1102-16. doi: 10.3389/fmicb.2021.635227

(3)Pautier P., Ribrag V., Duvillard P., Rey A., Elghissassi I., Sillet-Bach I., et al. Results of a prospective dose-intensive regimen in 27 patients with small cell carcinoma of the ovary of the hypercalcemic type. Ann Oncol. 2007;18(12):1985-9.

(4)Mittal, P. and Roberts, C.W.M. "The SWI/SNF complex in cancer - biology, biomarkers and therapy." *Nature reviews. Clinical oncology* vol. 17,7 (2020): 435-448. doi:10.1038/s41571-020-0357-3.

(5)Jones, C.A., Tansey, W.P., & Weissmiller, A.M. (2022). Emerging Themes in Mechanisms of Tumorigenesis by SWI/SNF Subunit Mutation. *Epigenetics insights*, *15*, 25168657221115656. https://doi.org/10.1177/25168657221115656

(6)Fahiminiya, S., Witkowski, L., Nadaf, J., Carrot-Zhang, J., Goudie, C., Hasselblatt, M., Johann, P., Kool, M., Lee, R. S., Gayden, T., Roberts, C. W., Biegel, J. A., Jabado, N., Majewski, J., & Foulkes, W. D. Molecular analyses reveal close similarities between small cell carcinoma of the ovary, hypercalcemic type and atypical teratoid/rhabdoid tumor. *Oncotarget*, *7*(2), 1732–1740. https://doi.org/10.18632/oncotarget.6459

(7) Pan J., McKenzie, Z.M., D'Avino A.R., Mashtalir, N., Lareau, C.A., St Pierre, R., Kadoch, C. The ATPase module of mammalian SWI/SNF family complexes mediate subcomplex identity and catalytic activity-independent genomic targeting. Nat Genet. 2019;51(4):618-26.

(8)Hoffman G.R., Rahal R., Buxton F., Xiang K., McAllister G., Frias, E., Bagdasarian, L., Huber J., Lindeman A., Chen D., Romero R., Ramadan N., Phadke T., Haas K., Jaskelioff M., Wilson B.G., Meyer M.J., Saenz-Vash V., Zhai H., Myer V.E., Porter J.A., Keen N., McLaughlin M.E., Mickanin C., Roberts C.W., Stegmeier F., Jagani Z. Functional epigenetics approach identifies BRM/SMARCA2 as a critical synthetic lethal target in BRG1-deficient cancers. Proc Natl Acad Sci U S A. 2014 Feb 25;111(8):3128-33. doi: 10.1073/pnas.1316793111. Epub 2014 Feb 11. PMID: 24520176; PMCID: PMC3939885.

(9)Orlando, K.A., Douglas, A.K., Abudu, A., Wang, Y., Tessier-Cloutier B., Su W., Weissman. Re-expression of SMARCA4/BRG1 in small cell carcinoma of the ovary, hypercalcemic type (SCCOHT) promotes an epithelial-like gene signature through AP-1-dependent mechanism, eLife. 2020;9.

(10)Moe, K.C., Maxwell, J.N., Wang, J., Jones, C.A., Csaki, G.T., Florian, A.C., Romer, A.S., Bryant, D.L., Farone, A.L., Liu, Q., Tansey, W.P., & Weissmiller, A.M. "The SWI/SNF ATPase BRG1 facilitates multiple pro-tumorigenic gene expression programs in SMARCB1-deficient cancer cells." *Oncogenesis* vol. 11,1 30. 1 Jun. 2022, doi:10.1038/s41389-022-00406-6

(11)Helming K.C., Wang X., Wilson B.G., Vazquez F., Haswell J.R., Manchester H.E., Kim Y., Kryukov G.V., Ghandi M., Aguirre A.J., Jagani Z., Wang Z., Garraway L.A., Hahn W.C., Roberts C.W. ARID1B is a specific vulnerability in ARID1A-mutant cancers. Nat Med. 2014 Mar;20(3):251-4. doi: 10.1038/nm.3480. Epub 2014 Feb 23. PMID: 24562383; PMCID: PMC3954704.

(12)Ozaki, T., and Nakagawara, A.. "Role of p53 in Cell Death and Human Cancers." *Cancers*vol. 3,1 994-1013. 3 Mar. 2011, doi:10.3390/cancers3010994

(13)Zhu, X., Liao, Y., & Tang, L. (2020). Targeting BRD9 for Cancer Treatment: A New Strategy. *OncoTargets and therapy*, *13*, 13191–13200. https://doi.org/10.2147/OTT.S286867

(14)Michel B.C., D'Avino A.R., Cassel S.H., Mashtalir N., McKenzie Z.M., McBride M.J., Valencia A.M., Zhou Q., Bocker M., Soares L.M.M., Pan J., Remillard D.I., Lareau C.A., Zullow H.J., Fortoul N., Gray N.S., Bradner J.E., Chan H.M., Kadoch C.. A non-canonical SWI/SNF complex is a synthetic lethal target in cancers driven by BAF complex perturbation. Nat Cell Biol. 2018 Dec;20(12):1410-1420. doi: 10.1038/s41556-018-0221-1. Epub 2018 Nov 5. PMID: 30397315; PMCID: PMC6698386.

(15)Zhang R., Xu W., Shao S., Wang Q. Gene Silencing Through CRISPR Interference in Bacteria: Current Advances and Future Prospects. Front. Microbiol.. 2021; 12. https://www.frontiersin.org/articles/10.3389/fmicb.2021.635227

(16)Kampmann, Martin. "CRISPRi and CRISPRa Screens in Mammalian Cells for Precision Biology and Medicine." *ACS chemical biology* vol. 13,2 (2018): 406-416. doi:10.1021/acschembio.7b00657

(17)Ying Y, Yang X, Zhao K, Mao J, Kuang Y, Wang Z, Sun R, Fei J. The Krüppel-associated box repressor domain induces reversible and irreversible regulation of endogenous mouse genes by mediating different chromatin states. Nucleic Acids Res. 2015 Feb 18;43(3):1549-61. doi: 10.1093/nar/gkv016. Epub 2015 Jan 21. PMID: 25609696; PMCID: PMC4330378.

(18)Alerasool N, Segal D, Lee H, Taipale M. An efficient KRAB domain for CRISPRi applications in human cells. Nat Methods. 2020 Nov;17(11):1093-1096. doi: 10.1038/s41592-020-0966-x. Epub 2020 Oct 5. PMID: 33020655.

(19)Eissenberg JC, Elgin SC. HP1a: a structural chromosomal protein regulating transcription. Trends Genet. 2014 Mar;30(3):103-10. doi: 10.1016/j.tig.2014.01.002. Epub 2014 Feb 17. PMID: 24555990; PMCID: PMC3991861.

(20)Kadoch, C., Hargreaves, D. C., Hodges, C., Elias, L., Ho, L., Ranish, J., & Crabtree, G. R. (2013). Proteomic and bioinformatic analysis of mammalian SWI/SNF complexes identifies extensive roles in human malignancy. *Nature genetics*, *45*(6), 592–601. https://doi.org/10.1038/ng.2628

(21)Mashtalir, N., D'Avino, A.R., Michel, B.C., Luo, J., Pan J., Otto J.E., Zullow H.J., McKenzie Z.M., Kubiak R.L., St Pierre R., Valencia A.M., Poynter S.J., Cassel S.H., Ranish J.A., Kadoch C. Modular Organization and Assembly of SWI/SNF Family Chromatin Remodeling Complexes. Cell. 2018 Nov 15;175(5):1272-1288.e20.

(22)Sanson K.R., Hanna R.E., Hegde M., Donovan K.F., Strand C., Sullender M.E., Vaimberg E.W., Goodale A., Root D.E., Piccioni F., Doench J.G. Nat Commun. 2018 Dec 21;9(1):5416. doi: 10.1038/s41467-018-07901-8.10.1038/s41467-018-07901-8 PubMed 30575746

(23)Westermann, L., Li, Y., Göcmen, B., Niedermoser, M., Rhein, K., Jahn, J., Cascante, I., Schöler, F., Moser, N., Neubauer, B., Hofherr, A., Behrens, Y. L., Göhring, G., Köttgen, A., Köttgen, M., & Busch, T. (2022). Wildtype heterogeneity contributes to clonal variability in genome edited cells. *Scientific reports*, *12*(1), 18211. https://doi.org/10.1038/s41598-022-22885-8

(24)Myrbråten, I. S., Wiull, K., Salehian, Z., Håvarstein, L. S., Straume, D., Mathiesen, G., & Kjos, M. (2019). CRISPR Interference for Rapid Knockdown of Essential Cell Cycle Genes in *Lactobacillus plantarum*. *mSphere*, *4*(2), e00007-19.

(25)Fu, Y., Foden, J., Khayter, C., Maeder, M., Reyon, D., Joung, J., Sander, J.. High-frequency off-target mutagenesis induced by CRISPR-Cas nucleases in human cells. *Nat Biotechnol* **31**, 822–826 (2013). https://doi.org/10.1038/nbt.2623